Applied Radiation and Isotopes 67 (2009) 39–45

Contents lists available at ScienceDirect

Applied Radiation and Isotopes

journal homepage: www.elsevier.com/locate/apradiso

Monte-Carlo simulations of elastically backscattered neutrons from hidden explosives using three different neutron sources

I. ElAgib [a,*], N. Elsheikh [b], H. AlSewaidan [a], F. Habbani [c]

[a] College of Science, King Saud University, P.O. Box 2455, Saudi Arabia
[b] College of Applied & Industrial Science, University of Juba, Khartoum, P.O. Box 321, Sudan
[c] Faculty of Science, Physics Department, University of Khartoum, Khartoum, P.O. Box 321, Sudan

ARTICLE INFO

Article history:
Received 16 June 2008
Received in revised form
13 July 2008
Accepted 15 July 2008

Keywords:
Landmines identification
Neutron backscattering
Monte-Carlo simulation

ABSTRACT

Calculations of elastically backscattered (EBS) neutrons from hidden explosives buried in soil were performed using Monte-Carlo N-particle transport code MCNP5. Three different neutron sources were used in the study. The study re-examines the performance of the neutron backscattering methods in providing identification of hidden explosives through their chemical composition. The EBS neutron energy spectra of fast and slow neutrons of the major constituent elements in soil and an explosive material in form of TNT have shown definite structures that can be used for the identification of a buried landmine.

1. Introduction

Civilian de-mining has become an urgent need in many former conflict areas around the world. The most common explosives used in landmines are TNT ($C_7H_5N_3O_6$) and RDX ($C_3H_6N_6O_6$). As their composition indicates, they are composed of four basic elements: hydrogen, carbon, nitrogen and oxygen. Although many organic materials buried in soil are also composed of the same elements, use can be made of the fact that explosives have concentrations that are different than in soil and in most common organic materials. One way for the detection and identification of explosives is the use of neutrons. Several investigations were carried out on the advantages and limitations of neutron-based techniques used for the detection and identification of anti-personnel landmines (e.g. Csikai and ElAgib, 1999; ElAgib and Csikai, 1999; Datema et al., 2000; Hussein and Waller, 2000; Kiraly et al., 2001; Brooks et al., 2004). The incident neutrons will interact with the nuclei of the major chemical elements in the mine (H, C, N and O), emitting elastically backscattered fast and thermal neutrons spectra which can act as fingerprints of these chemical elements. The EBS neutrons can be detected by a suitable detector capable of differentiating the EBS neutrons according to their energy and their flux. The concentration of hydrogen, carbon, nitrogen or oxygen can be evaluated by calculating the EBS net relative yield of the neutrons and observing the different patterns of their energy spectra (Hussein, et al., 2005). One other detection approach based on neutron backscattering is to simply detect the hydrogen content in soil by measurement of thermal backscattered neutrons from hidden explosives. The change in hydrogen concentration in soil can be made by calculating the intensity of low-energy neutrons reflected back from soil (Hussein and Waller, 2000). The chemical elements of interest for the detection of explosives require neutron sources of different energies in order to be observed. Hydrogen is best observed through nuclear reactions initiated

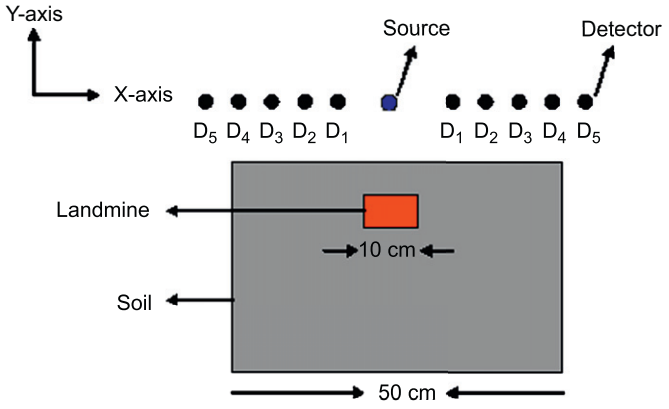

Fig. 1. Geometry used in the MCNP simulations.

* Corresponding author. Fax: +966 1 4676379.
E-mail address: elagib@ksu.edu.sa (I. ElAgib).

0969-8043/$ - see front matter © 2008 Elsevier Ltd. All rights reserved.
doi:10.1016/j.apradiso.2008.07.016

from very-low-energy neutrons. Other elements such as C, N, and O require neutron energies of several MeV to be observed. To satisfy this, the required neutron source should produce high-energy neutrons for the detection of elements such as C, N, and O, and low-energy neutrons for elements such as H (Vourvopoulos and Sullivan, 2006). Such a task can be accomplished with the use of a spontaneous fission source such as Cf-252 as well as (α, n) sources such as Pu–Be and Am–Be. These three isotopic neutron sources were used in the present study. The present work was done by considering a simple sample–source–detector geometry, simulating the EBS (fast and thermal) neutrons from the constituent elements of the explosive material and studying the variation in the net flux with the source energy spectrum. Such geometry was chosen in order to tally the EBS fast and thermal neutrons spectra at different angles. Moreover, it was considered simulating a practical situation.

Table 1
Composition of soil and TNT explosive as modeled in MCNP simulation (Hussein et al., 2005; Maucec and Rigollet, 2004)

Material/mass density ($g\,cm^{-3}$)	Elemental mass fraction/mass density ($g\,cm^{-3}$)					
	H	C	N	O	Si	Al
Soil	0.0146			0.5520	0.3607	0.0731
1.12	0.016			0.618	0.404	0.082
TNT ($C_7H_5N_3O_6$)	0.0217	0.370	0.1853	0.4229		
1.65	0.0358	0.610	0.306	0.689		

2. MCNP modeling

Monte-Carlo simulation of a landmine localization device using the neutron backscattering method was reported by Datema et al. (2002). The general-purpose Monte-Carlo N-particle (MCNP) code, as described by the X-5 Monte Carlo Team (2003), was used in the present study. The code accounts for all neutron reactions given in a particular cross-section evaluation (such as ENDF/B-VI). The evaluated data are processed into a format appropriate for MCNP with the help of codes such as NJOY (MacFarlane et al., 1982). Continuous nuclear cross-section data based on the ENDF/B-VI were used in the present computations. The net EBS neutron spectra were computed for the major elements of a landmine when buried in soil. Calculations were performed using a fixed point source with enough histories to have the statistical error less than 2% in all energy bins.

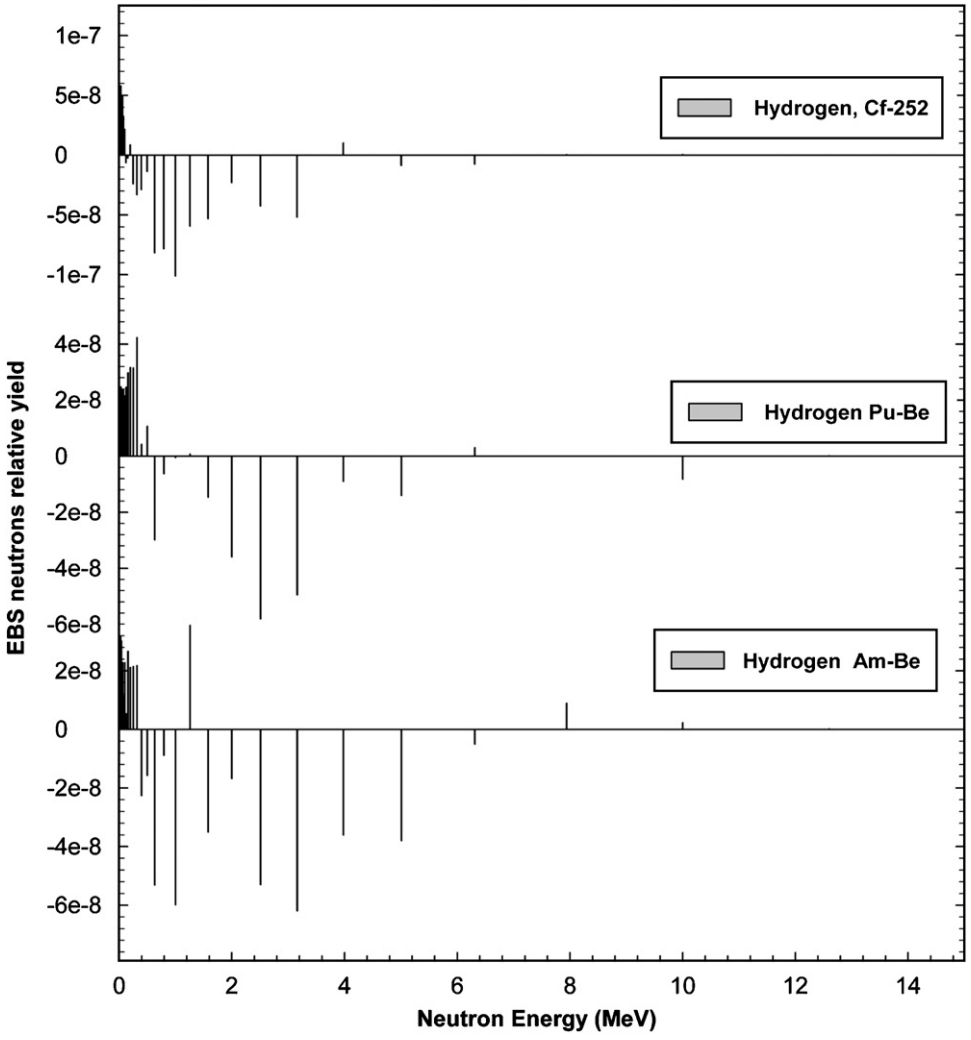

Fig. 2. The EBS neutron energy spectra from H for Cf-252, Pu–Be and Am–Be neutrons.

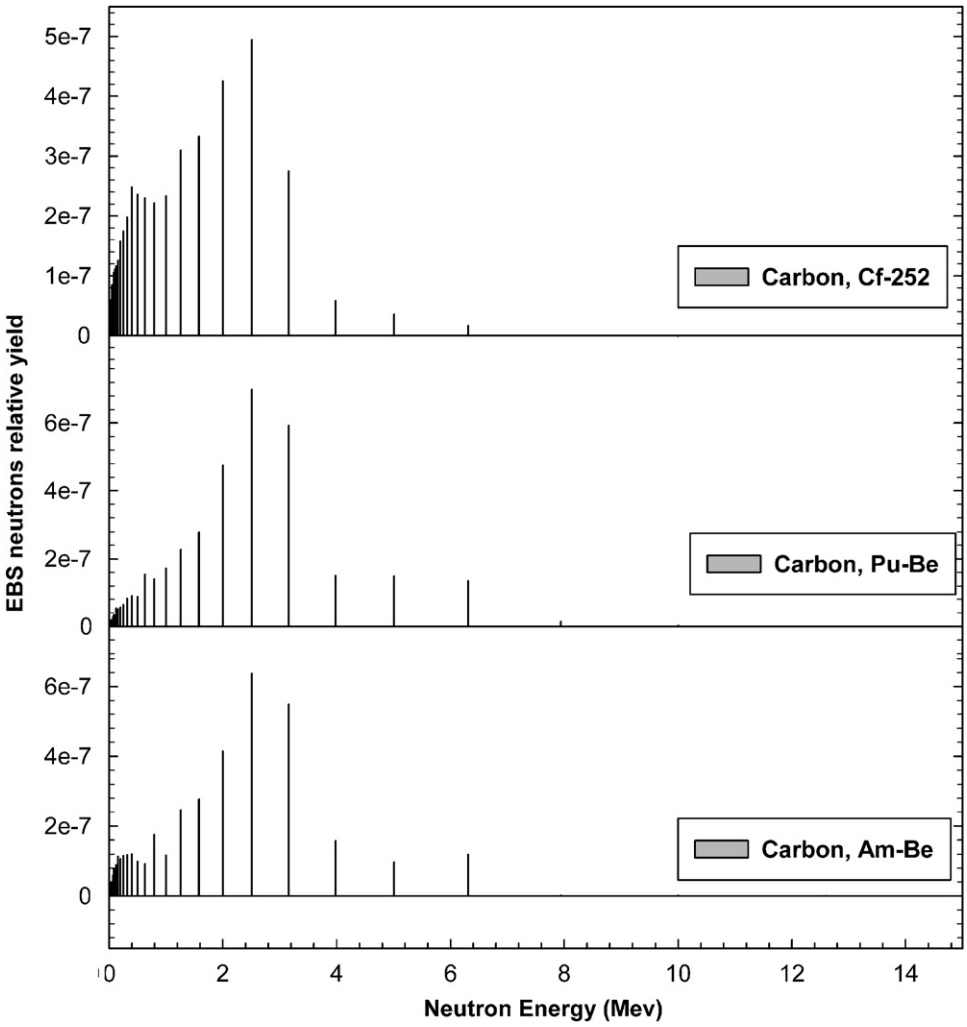

Fig. 3. The EBS neutron energy spectra from C for Cf-252, Pu–Be and Am–Be neutrons.

The sample–source–detector geometry used in the present study is shown in Fig. 1. The assumed model consists of soil of dimensions 50 cm × 50 cm × 50 cm, with the sample as an explosive material in the form of TNT of dimensions 10 cm × 10 cm × 10 cm, situated 5 cm deep in soil. Three different point neutron isotopic sources were used in the study: Cf-252, Pu–Be, and Am–Be. The sources were located vertically above the soil at $y = 10$ cm and $y = 20$ cm along the y-axis. Measured and normalized neutron spectra of Cf-252, Pu–Be, and Am–Be that were employed in the calculations were taken from Griffith et al. (1990). For each source position along the y-axis, a detector was located at 10 different points along the x-axis, on both sides of each source (i.e. at $x = \pm 10, \pm 15, \pm 20, \pm 25, \pm 30$ cm) in order to tally the EBS neutrons from the major constituent elements of the hidden explosive. The net EBS neutrons spectra were calculated by subtracting the background spectrum (soil) from the signal (soil and sample). The composition of soil and TNT explosive as modeled in the MCNP simulations is shown in Table 1, with the data taken from Maucec and Rigollet (2004) and Hussein et al. (2005). Mass densities (in g cm^{-3}) of H (0.02), C (2.23), N (0.81), O (1.14) and Si (2.33), that were used in the MCNP simulations, were taken from the same sources.

In the MCNP modeling two processes are allowed, inelastic and elastic treatments. For the inelastic treatment, the distribution of secondary energies is represented by a set of equally probable final energies for each member of a grid of initial energies from an upper limit of typically 4 eV down to 10^{-5} eV, along with a set of angular data for each initial and final energy, which was not considered in the present calculation. In the present simulation elastic scattering treatment was chosen with probability $\sigma el/(\sigma el+\sigma in)$.

3. Results and discussion

The net EBS neutron energy spectra from H, C, N and O, using Cf-252, Pu–Be and Am–Be neutron point sources located at 10 cm along the y-axis and a point detector located at ±10 cm beside the source along the x-axis, are shown in Figs. 2–5, respectively.

Fig. 2 represents the net EBS neutron energy spectra from H for Cf-252, Pu–Be and Am–Be neutron sources. In case of Cf-252, a few peaks of thermal elastically backscattered (TEBS) neutrons are observed in the thermal neutron energies from an upper limit 0.063 MeV and a lower limit 0.013 MeV, while for Pu–Be and Am–Be positive indications are observed in the thermal neutron energy range with upper limit 0.794 MeV. Relatively higher peaks of TEBS neutrons are observed in case of Pu–Be when

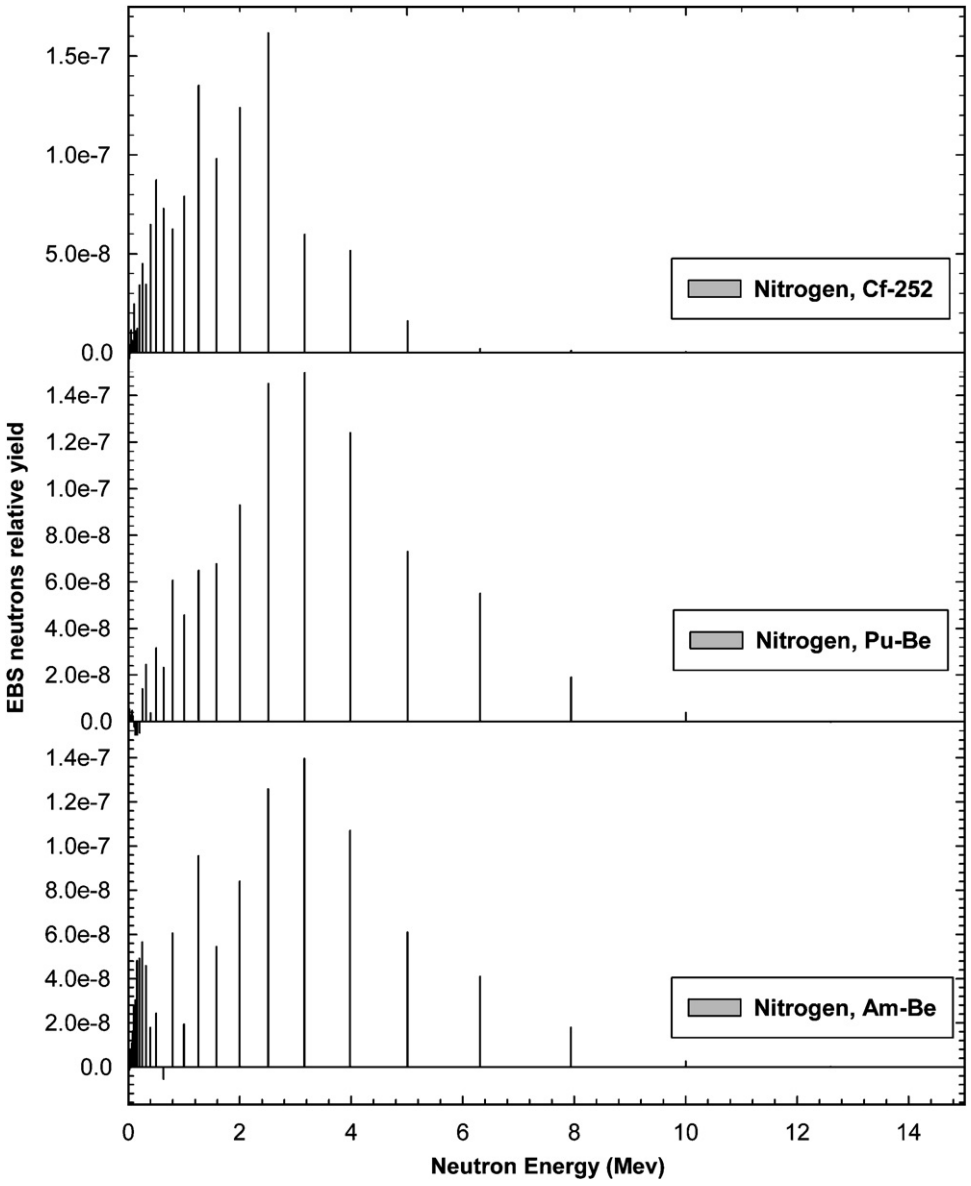

Fig. 4. The EBS neutron energy spectra from N for Cf-252, Pu–Be and Am–Be neutrons.

compared with Cf-252 and Am–Be neutron sources. The negative indications observed are from the soil, because fast elastically backscattered (FEBS) neutrons are higher from the constituent elements of soil. This behavior can be attributed to the moderating power of hydrogen in slowing down fast neutrons to thermal regions.

The net EBS neutron energy spectra from C for Cf-252, Pu–Be and Am–Be neutron sources are shown in Fig. 3. In case of Cf-252, more relatively high peaks of TEBS neutrons are observed at the low neutron energies with upper limit 0.794 MeV, when compared with H, while for Pu–Be and Am–Be, a few and relatively small peaks are observed at the slow neutron energy range 0.013–0.794 MeV. Relatively higher peaks of FEBS neutrons are observed at the energies 2.0, 2.51 and 3.16 MeV. In addition, relatively smaller peaks of FEBS neutrons are observed at the energies 3.98, 5.01 and 6.31 MeV for both Pu–Be and Am–Be neutron sources. This is reasonable, since C is less effective as a moderator compared to hydrogen.

The net EBS neutron energy spectra from N for Cf-252, Pu–Be and Am–Be neutrons are shown in Fig. 4. In case of Cf-252, intensive peaks of TEBS neutrons are observed at the low neutron energy range 0.013–0.794 MeV. Relatively high peaks of FEBS neutrons are also observed at energies 1.26, 2.0, 2.51, 3.16 and 3.98 MeV. More additional peaks are observed at energies 5.01, 6.31 and 7.94 MeV for both Pu–Be and Am–Be sources. Lower peaks are observed in case of nitrogen when compared with carbon.

Fig. 5 shows the net EBS neutron energy spectra from O for Cf-252, Pu–Be and Am–Be neutrons. A high peak of TEBS neutrons is observed at 0.794 MeV in the case of the three sources. Intensive peaks of TEBS neutrons are observed in case of Cf-252 when compared with Pu–Be and Am–Be neutron sources. Relatively high peaks of FEBS neutrons are observed at energies 2.51 and 3.16 MeV in case of Pu–Be and Am–Be when compared with Cf-252. More peaks of FEBS are observed at the energies 3.98, 5.01 and 6.31 MeV of Pu–Be and Am–Be neutrons.

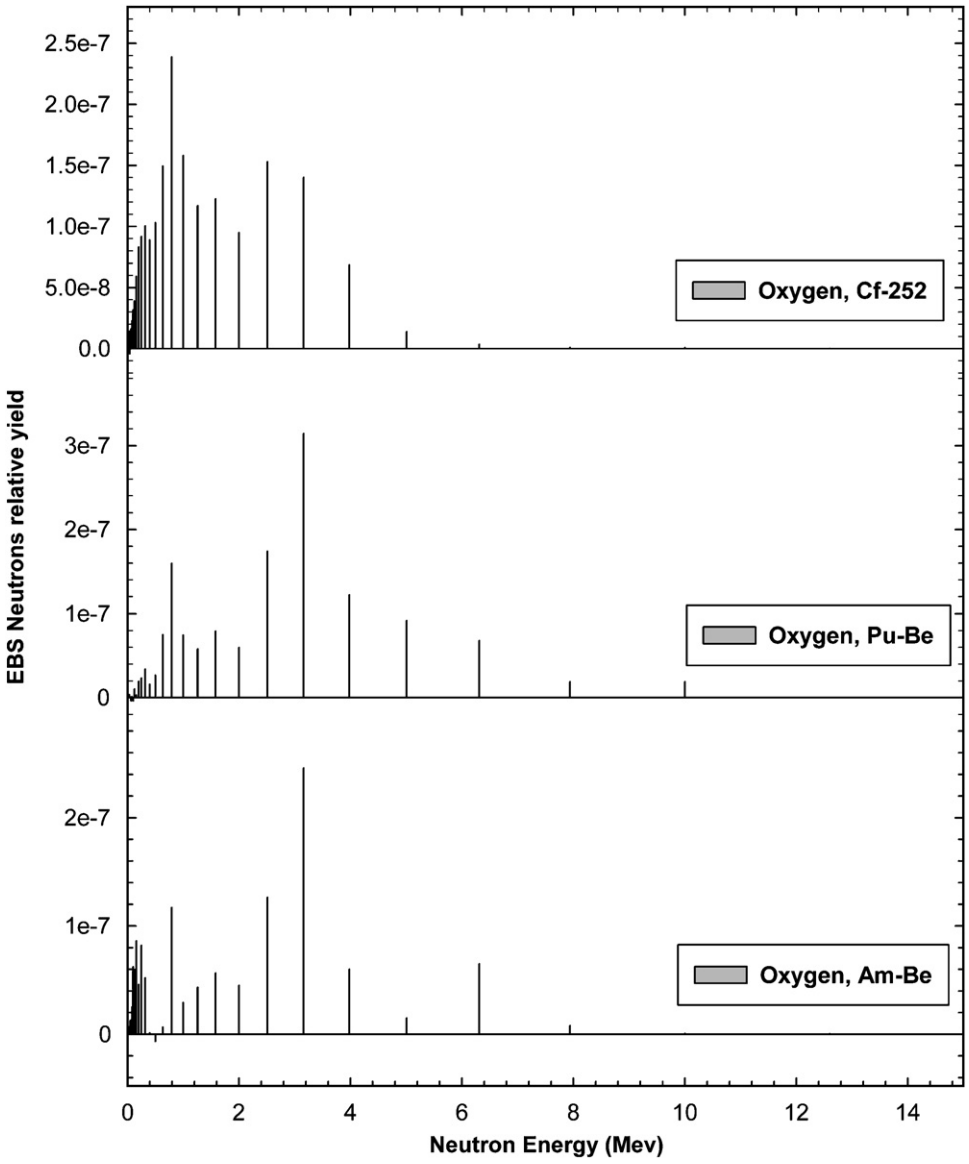

Fig. 5. The EBS neutron energy spectra from O for Cf-252, Pu–Be and Am–Be neutrons.

Fig. 6 represents the net EBS neutron energy spectra from landmine for Cf-252, Pu–Be, and Am–Be neutrons. In case of Cf-252, relatively high peaks of TEBS neutrons are observed at energies 0.316, 0.501 and 0.794 MeV. In addition, relatively higher peaks of FEBS neutrons are observed at 3.16 MeV. More additional peaks of FEBS neutrons are observed at energies 2.51, 5.01 and 6.3 MeV for the three sources, and more peaks are observed at 7.94 and 10 MeV in case of Cf-252 neutron source.

Peak ratios of the net EBS relative neutrons yield from landmine to the net EBS relative neutrons yield from soil were obtained at selected neutron energies. The variation of the peak ratios with neutron energy at $y = 10$ cm and $y = 20$ cm showed a similar pattern, with greater values obtained at $y = 20$ cm. Peak ratios at the lower neutron energies such as 0.079 and 0.316 MeV can be used for landmine identification with the TEBS neutrons-based method, while peak ratios at the higher neutron energies such as 1.0, 2.5, 3.16, 5.0 and 6.3 MeV can be used for landmine identification with the FEBS neutrons-based method.

The ratios of the net EBS spectral neutrons yield from landmine to the net EBS spectral neutrons yield from soil obtained at different detector positions ($x = \pm 10$, ± 15, ± 20, 6 ± 25, ± 30 cm), at two source positions ($y = 10$ cm, $y = 20$ cm) and for the Cf-252, Pu–Be and Am–Be neutron sources are shown in Fig. 7. It can be seen that the ratio of the EBS spectral neutrons yield is sensitive to the source and detector positions, and decreases as the source and detector positions are increased.

It is clear from the above results that the EBS neutrons spectra are spread throughout the slow and fast neutron energy regions. Effective detection of such neutron yields can be achieved by employing a detector capable of detecting both slow and fast neutrons.

4. Conclusion

In the present work, the Monte-Carlo simulations of EBS neutrons of Cf-252, Pu–Be and Am–Be neutron sources from the major constituent elements of landmine and soil were studied. The EBS neutron energy spectra of fast and thermal neutrons of the major constituent elements in soil and landmine have shown

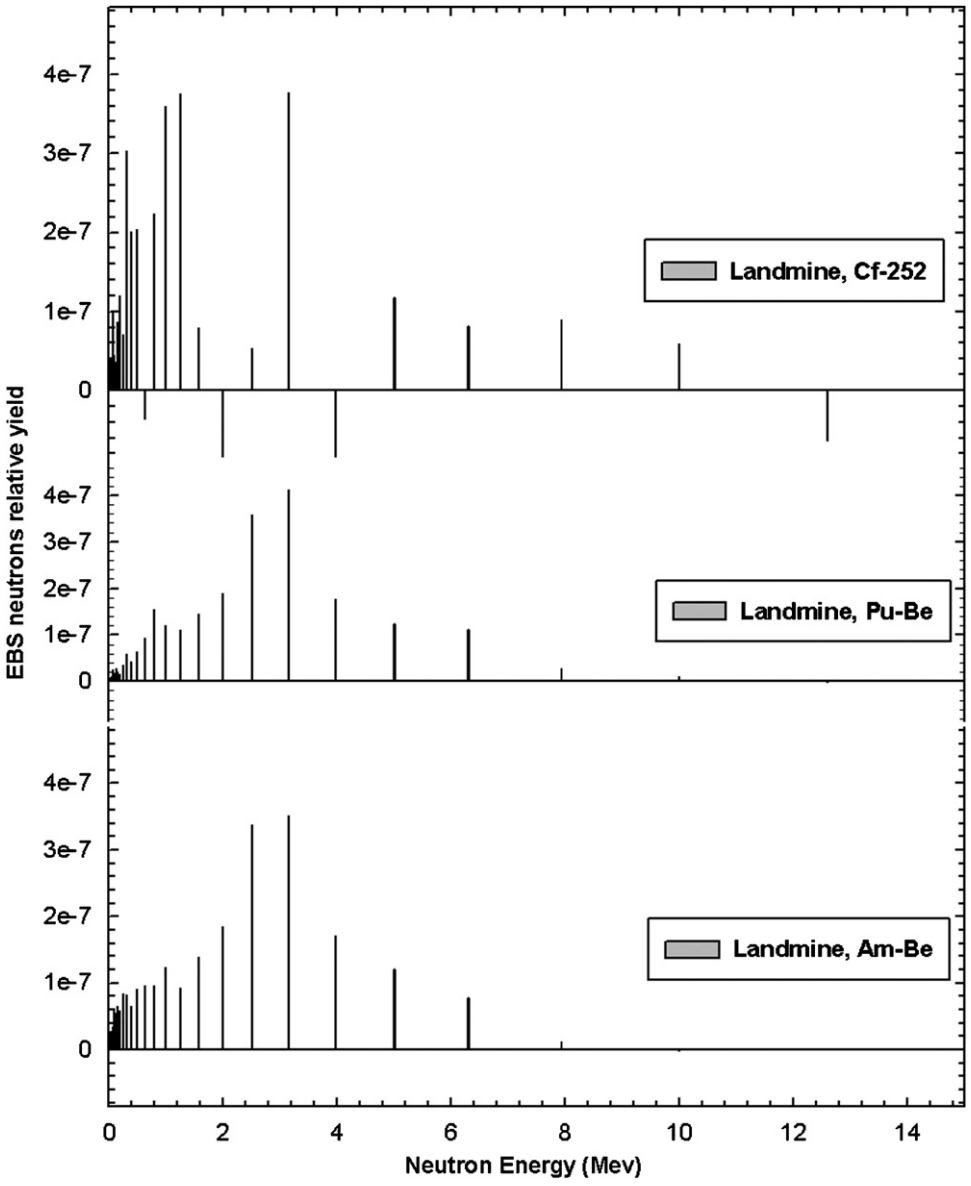

Fig. 6. The EBS neutron energy spectra from landmine for Cf-252, Pu–Be and Am–Be neutrons.

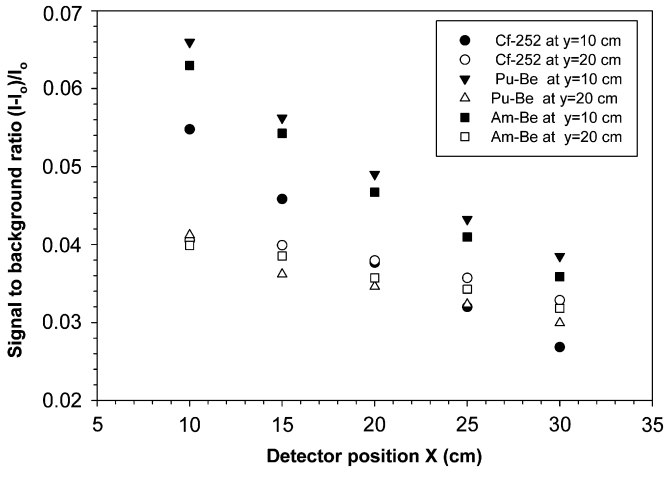

Fig. 7. EBS spectral neutrons relative yield of landmine to EBS spectral neutrons relative yield of soil ratio at different detector and source positions for Cf-252, Pu–Be and Am–Be neutron sources.

definite structures. It is found that it is possible to observe the EBS neutrons from hidden explosives, at different detector positions up to 30 cm away from the source, with source positions from 10 to 20 cm above the soil.

Acknowledgements

The authors are grateful for the support granted within the Project (Phy/2005/350), financed by the Research Center, College of Science, King Saud University, Saudi Arabia.

References

Brooks, F.D., Buffer, A., Allie, M.S., 2004. Detection of anti-personnel landmines using neutrons and gamma-rays. Radiat. Phys. Chem. 71, 749–757.

Csikai, J., ElAgib, I., 1999. Bulk media assay using backscattered Pu–Be neutrons. Nucl. Instrum. Methods A 432, 410–414.

Datema, C.P., Bom, V.R., Van Eijk, C.W.E., 2000. Landmine detection with the neutron backscattering method. IEEE Nucl. Sci. Conf. Record 1, 5111–5114.

Datema, C.P., Bom, V.R., Van Eijk, C.W.E., 2002. Experimental results and Monte Carlo simulations of a landmine localization device using the neutron backscattering method. Nucl. Instrum. Methods A 488, 441–450.7.
ElAgib, I., Csikai, J., 1999. Validation of neutron data libraries by backscattered spectra of Pu–Be neutrons. Nucl. Instrum. Methods A 435, 456–461.
Griffith, R.V., Palfalvi, J., Madhvanath, U., 1990. Compendium of neutron spectra and detector responses for radiation protection purposes. IAEA Technical Report Ser. No. 318, IAEA, Vienna.
Hussein, E.M.A., Waller, E.J., 2000. Landmine detection: the problem and the challenge. Appl. Radiat. Isot. 53 (4–5), 557–563.
Hussein, E.M.A., Desrosiers, M., Waller, E.J., 2005. On the use of radiation scattering for the detection of landmines. Radiat. Phys. Chem. 73, 7–19.
Kiraly, B., Olah, L., Csikai, J., 2001. Neutron-based techniques for detection of explosives and drugs. Radiat. Phys. Chem. 61, 781–784.
MacFarlane, R.E., Muir, D.W., Boicourt, R.M., 1982. The NJOY nuclear data processing system: users manual. Los Alamos National Laboratory Report LA-9303-M, vol. I (ENDF-324).
Maucec, M., Rigollet, C., 2004. Monte Carlo simulations to advance characterization of landmines by pulsed fast/thermal neutron analysis. Appl. Radiat. Isot. 61, 35–42.
Vourvopoulos, G., Sullivan, R.A., 2006. Evaluation of PELAN as a landmine confirmation sensor. In: Proceedings of the SPIE, International Society for Optical Engineering, 6217 I, Art. No. 62171P.
X-5 Monte Carlo Team, 2003. MCNP—A General Monte Carlo N-Particle Transport Code: Overview and Theory, V. 5, vol. 1, Los Alamos National Laboratory.